PHOTONICS Research

Excellent light-capture capability of trilobal SiNW for ultra-high J_{SC} in single-nanowire solar cells

Zhongliang Gao,[1] Guilu Lin,[2] Yupeng Zheng,[1] Na Sang,[2] Yingfeng Li,[1] Lei Chen,[2] and Meicheng Li[1,*]

[1]State Key Laboratory of Alternate Electrical Power System with Renewable Energy Sources, School of Renewable Energy, North China Electric Power University, Beijing 102206, China
[2]School of Mathematics and Physics, North China Electric Power University, Beijing 102206, China
*Corresponding author: mcli@ncepu.edu.cn

Received 13 December 2019; revised 9 February 2020; accepted 9 March 2020; posted 9 March 2020 (Doc. ID 385867); published 1 June 2020

Single-nanowire solar cells with a unique light-concentration property are expected to exceed the Shockley–Queisser limit. The architecture of single nanowire is an important factor to regulate its optical performance. We designed a trilobal silicon nanowire (SiNW) with two equivalent scales that possesses superior light-absorption efficiency in the whole wavelength range and shows good tolerance for incident angle. The electric field distribution in this geometry is concentrated in the blade with small equivalent scale and pivot with large equivalent scale, respectively, in the short wavelength range and long wavelength range. Corresponding good light absorption of trilobal SiNW in the two wavelength ranges leads to stronger total light-absorption capacity than that of cylindrical SiNW. Trilobal single-nanowire solar cells can obtain a short-circuit current density (J_{SC}) of 647 mA · cm^{-2}, which provides a new choice for designing single nanowire with excellent light-capture capability.

https://doi.org/10.1364/PRJ.385867

1. INTRODUCTION

Nanowires have attracted extensive attention and research due to their special properties, such as good elasticity, large specific surface area, and particular photoelectric effect [1–5]. The excellent light-capture capability endows nanowires with great application potential in the field of high-efficiency and low-cost photovoltaic devices [6,7]. Single or multiple single nanowires with a small footprint can be integrated into optoelectronic/optical subsystems for future on-chip as low-power energy nanogenerators, which are interesting components of small photovoltaics [8,9]. Compared with nanowire array solar cells, single-nanowire solar cells can simplify analyses by removing the ensemble averaging effect and nonuniform contacting effect and will get more accurate study of its performance [10–14]. Single-core-shell p-i-n junction GaAs nanowire solar cells with unique light-concentration property achieve an ultra-high short-circuit current density (J_{SC}) of 180 mA · cm^{-2}, which leads to an apparent solar efficiency above the Shockley–Queisser limit [6].

The amount of light absorption is of great importance to solar cells, because it determines the maximum power output of the solar cells [15]. Nanowires with a unique light-concentration property can reduce the materials consumption and the space occupation of the device, which can directly affect the design and preparation of devices [9,16]. The light absorption of single nanowire is a complex process that mainly depends on the cross-section shape, height of the nanowire, refractive index of the environmental medium, and the angle of incident light [16–19]. Cylindrical nanowire is one of the most commonly used nanowire types in many fields [5,9,10,16,17]. This nanowire has a sharp optical resonance peak with strong intensity and narrow width, which can only achieve high-efficiency light absorption at the optical resonance peak position [20–22]. There is a corresponding relationship between the diameter of cylindrical nanowire and the position of the optical resonance peak [23]. To improve the light-absorption efficiency in the whole wavelength range, we can increase the number of optical resonance peaks by adjusting the geometry of nanowire, such as funnel-shaped and conical silicon nanowire (SiNW) with several equivalent diameters [24–27].

In this work, we design a trilobal SiNW model with two equivalent scales that has superior light-absorption efficiency in the wavelength range of 0.3–0.6 μm. The total light absorption of the trilobal SiNW is more than that of the cylindrical SiNW. Meanwhile, it has a good tolerance to the incident angle, which reduces the influence of incident angle on light absorption. Trilobal single-SiNW solar cells can obtain a J_{SC} of 647 mA · cm^{-2} due to their excellent light-capture capability.

2. METHODS

A. Design of SiNW Models

A schematic diagram of the fabrication of the trilobal SiNW is shown in Fig. 1. The top view shows the trilobal SiNW takes

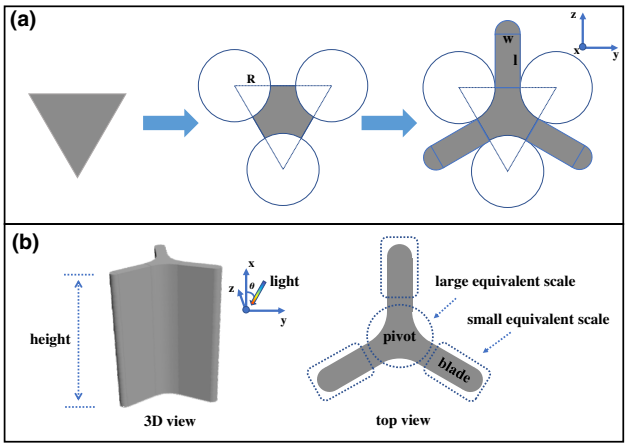

Fig. 1. Schematic diagram of trilobal SiNWs. (a) Assembly process, geometric relationship of top view, and (b) 3D view and top view with different equivalent scales.

the difference set of an equilateral triangle and three circles and then merges with a rectangle and semicircle on three sides, where the side length of the equilateral triangle is a, the radius of the big circle is R, the length of the rectangle is l, and the diameter of the small circle is w, which is the width of the rectangle. Here, a is fixed at 60 nm and l is fixed at 50 nm. The top view of the cylindrical SiNW is a circle, where the diameter of the circle is d. The comparison of the optical properties of two models uses the same volumes and different geometries; the parameters are shown in Table 1.

B. Calculation Methods

All of our optical calculations are performed using the software package Discrete Dipole Approximation Code (DDSCAT 7.3). This software package is based on DDA theory, which is a freely available open-source Fortran-90 software package [28–30]. It can be used to study absorption, scattering, extinction, and light fields distribution around nanostructures, and we have verified the accuracy of the calculation in the previous work [31]. In this approximation, the model is replaced by an array of point dipoles. This process is realized by self-programming language MATLAB. It is found that the vertical structure of the single-nanowire solar cells is in the medium [6], where the refractive index of ambient medium was set to 1.284. The computational domain of near field is a rectangular volume whose center coincides with that of the physical model. Its height, width, and length are set as 3 times, 2 times, and 2 times of physical model height, width, and length, respectively. The incident direction of light is in the xy plane, as shown in Fig. 1(b). The polarization direction of the incident light has been studied in trilobal SiNW. When the incident light is perpendicular to the trilobal SiNW, the polarization direction has little effect on light-absorption spectra, because the trilobal SiNW is axisymmetric. Here, the default polarization direction of 90° is perpendicular to the incident light in the xy plane, which is used in the following calculations.

Table 1. Geometric Parameters of Trilobal and Cylindrical SiNWs

	Trilobal SiNW		Cylindrical SiNW		
Serial Number	Width[a] (nm)	Height (μm)	Diameter[a] (nm)	Height (μm)	Cross Section[a] (nm^2)
1	10	0.3	62	0.3	3019
2	15	0.3	68	0.3	3631
3	20	0.3	74	0.3	4300
4	25	0.3	80	0.3	5026
5	15	0.1	68	0.1	3631
6	15	0.3	68	0.3	3631
7	15	0.5	68	0.5	3631
8	15	0.7	68	0.7	3631

[a]Widths, diameters, and cross sections are accurate to the integer bit.

The absorption efficiency and extinction efficiency are used to measure the light-capture capability of nanowires. The absorption efficiency is defined as the ratio of the light-absorption cross section (σ_{abs}) to the geometric cross section (σ_{geom}). The σ_{abs} of nanowires is usually larger than its σ_{geom}, which indicates that is has the ability of optical concentration. We calculated the light-absorption spectral power (A) and total light absorption (A_τ) under the AM 1.5 G solar spectrum [32]:

$$A(\lambda) = [\sigma_{abs}(\lambda)/\sigma_{geom}] \times I(\lambda), \tag{1}$$

$$A_\tau = \int_{\lambda_{min}}^{\lambda_{max}} A(\lambda) d\lambda, \tag{2}$$

where λ is wavelength, λ_{min} and λ_{max} are 0.3 and 1.1 μm, respectively, and I is the irradiance under the AM 1.5 G solar spectrum. The obtainable J_{SC} can be calculated by

$$J_{SC} = q \int_{\lambda_{min}}^{\lambda_{max}} A(\lambda) \frac{\lambda}{hc} d\lambda, \tag{3}$$

where q is elementary charge, h is Planck's constant, and c is the speed of light in vacuum.

3. RESULTS AND DISCUSSION

There is a consistent correlation between optical resonance and cutoff wavelength according to the leaky mode theory, which can be calculated in infinite cylindrical SiNW by the equation

$$V = \frac{\pi d}{\lambda \sqrt{n^2 - 1}}, \tag{4}$$

where V is the cutoff parameter that depends on the waveguide mode, d is the diameter of the cylindrical SiNW, and n is the refractive index of silicon [23]. Based on the leaky mode theory, we obtained an exact comprehensive equation,

$$\lambda = A - Bh + Cd + Dhd + Ed^2, \tag{5}$$

for cylindrical SiNW in our previous work, where h is the height of the cylindrical SiNW, and A–E are undetermined coefficients and can be determined by a regression approach [23]. The diameter determines the position of the optical resonance peak and height determines the intensity of the optical resonance peak. A conical SiNW with five equivalent diameters has been designed, and optical resonance peaks at different positions have been obtained [25]. However, the total light absorption of conical SiNW is lower than that of cylindrical

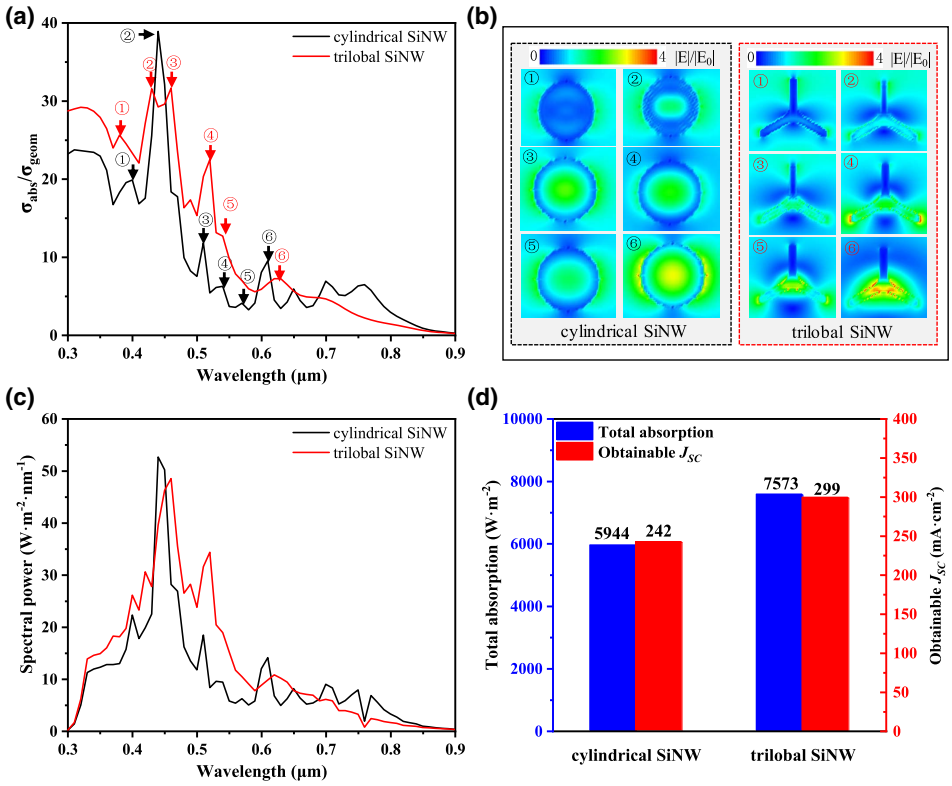

Fig. 2. (a) Absorption efficiency, (b) electric field distribution in *yz* plane, (c) light-absorption spectral power under AM 1.5 G solar spectrum, and (d) total absorption and obtainable J_{SC} with cylindrical and trilobal SiNWs with the same cross section of 3631 nm^2 and height of 0.3 μm.

SiNW, because these equivalent diameters with short height reduce the light-absorption efficiency.

To achieve several optical resonance peaks for broadening the absorption spectrum and improving the optical capture capacity, a trilobal SiNW with two equivalent scales was designed. Its top view shows that the blade is a small equivalent scale and the pivot is a large equivalent scale, and the three-dimensional (3D) view shows that different equivalent scales have the same height, as shown in Fig. 1(b). The blades have optical resonance peaks in the short wavelength range, the pivot has optical resonance peaks in the long wavelength range, and different equivalent scales with the same height ensure the intensity of optical resonance peaks, which gives the trilobal SiNW strong light-capture capability.

The cylindrical SiNW has only one strong optical resonance peak, and others are weak, as shown in Fig. 2(a), because the top view has only one equivalent scale. Figure 2(b) shows that electric fields at different optical resonance peaks ($\lambda = 0.4$, 0.44, 0.51, 0.57, 0.61 μm) are concentrated in the center of the cylindrical SiNW, and those of the trilobal SiNW at optical resonance peaks ($\lambda = 0.38$, 0.43, 0.46, 0.52, 0.54, 0.63 μm) are different due to its two equivalent scales. The blades with small equivalent scale correspond to optical resonance peaks in the short wavelength range ($\lambda \le 0.46$ μm), where the electric field is concentrated in the blades. There are electric field distractions at both blade and pivot of the trilobal SiNW in the medium wavelength range (0.46 μm $\le \lambda \le$ 0.54 μm), which shows that both equivalent scales have optical resonance peaks in the medium wavelength range. The pivot of the trilobal SiNW with large equivalent scale corresponds to optical resonance peaks in the long wavelength range ($\lambda \ge 0.54$ μm), where the electric field is concentrated in the pivot. This shows that the electric field moves from the small equivalent scale to the large equivalent scale with the increase of wavelength. Absorption efficiency of the trilobal SiNW in the wavelength range of 0.3–0.43 μm and 0.46–0.59 μm is stronger than that of the cylindrical SiNW. Therefore, the trilobal SiNW has strong optical resonance in those wavelength ranges due to its different equivalent scales.

The total light absorption in solar cells should consider the absorption efficiency under the solar spectrum, because the irradiance is not evenly distributed at different wavelengths. In the wavelength range of 0.3–0.33 μm, the absorption efficiency spectrum of trilobal SiNW is higher than that of the cylindrical SiNW, but the spectral power is almost equal, as shown in Fig. 2(c), because the irradiance in this wavelength range is weak. To improve the total light absorption, the absorption efficiency should be improved at the high irradiance position. For the trilobal SiNW, the absorption efficiency is higher in the wavelength range of 0.3–0.6 μm, including the position with higher irradiance at $\lambda = 0.5$ μm in the solar spectrum. The spectral power of the trilobal SiNW is higher than that of the cylindrical SiNW in wavelength ranges of 0.33–0.43 μm and 0.45–0.59 μm, with the same cross section of 3631 nm^2 and height of 0.3 μm. Figure 2(d) shows the total light absorption and obtainable J_{SC}, where the obtainable J_{SC}

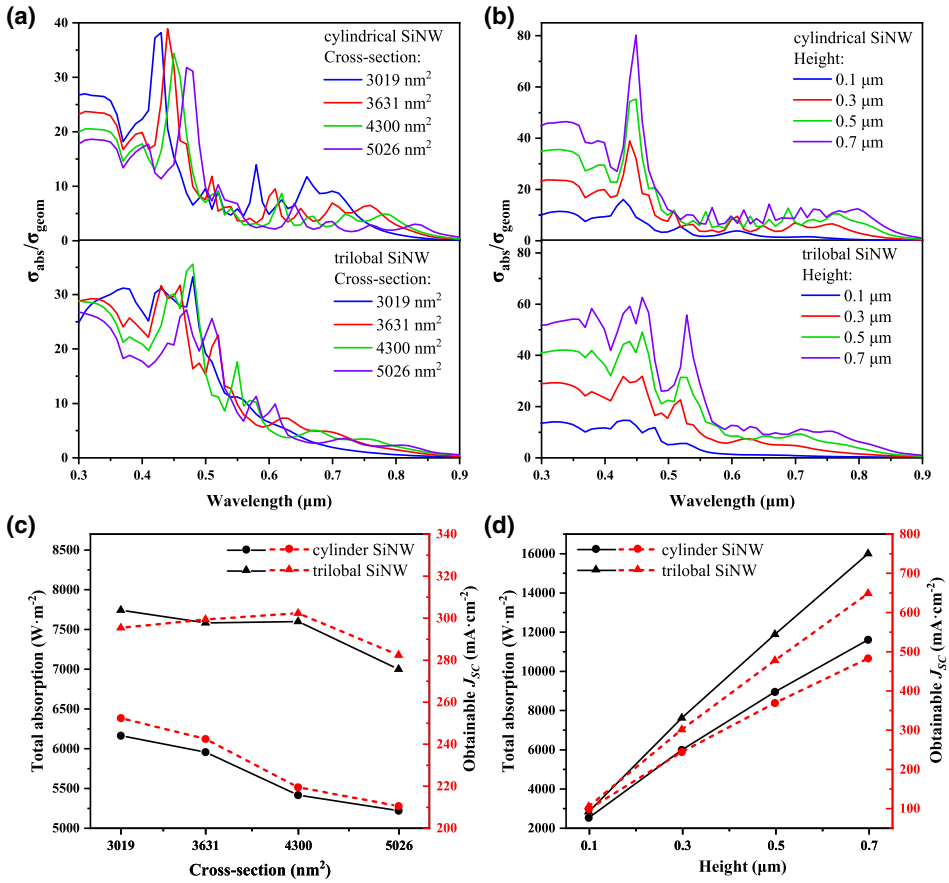

Fig. 3. Absorption efficiency of cylindrical and trilobal SiNWs with different (a) cross sections and (b) heights. The change of the cross section is through changing the diameter of the cylindrical SiNW and the width of the blade of the trilobal SiNW. Total absorption and obtainable J_{SC} of cylindrical and trilobal SiNWs with different (c) cross sections and (b) heights.

of the cylindrical single-SiNW solar cells is 242 mA · cm^{-2}, which is reliable, according to previous research [6,33]. The light absorption of the trilobal SiNW is 7573 W · m^{-2}, 1629 W · m^{-2} higher than that of the cylindrical SiNW, and the obtainable J_{SC} is 299 mA · cm^{-2}, 57 mA · cm^{-2} higher than that of the cylindrical SiNW.

Figure 3(a) shows that optical resonance peaks of the cylindrical SiNW are redshifted with the increase of diameter, and the total absorption and obtainable J_{SC} are reduced because its equivalent scale gradually increases. The change of cross section is through changing of the width of the trilobal SiNW blades in Fig. 3(a). The relationship between cross section and width is shown in Table 1. The width of the blades of the trilobal SiNW has a great influence on the optical resonance in the wavelength range of 0.3–0.46 μm according to the electric field distraction in Fig. 2(b). The absorption efficiency decreases when the blade width increases, as shown in Fig. 3(a), because the increase of blade equivalent scale makes the resonance wavelength range change. However, there are some redshifts in the absorption efficiency spectra due to the increase of blade width, when whole equivalent scale of the trilobal SiNW becomes larger. The trilobal SiNW with two equivalent scales can adjust the intensity of absorption efficiency spectra in the wavelength range of 0.3–0.46 μm by controlling the blade width. The relationship between the absorption efficiency spectra and geometric parameters is the same as expected in the model design. Figure 3(c) shows that the total light absorption decreases and obtainable J_{SC} first increases a little, then decreases with the increase of blade width. The total light absorption and obtainable J_{SC} are always more than that of the cylindrical SiNW with the same cross section.

Figure 3(b) shows that the relationship between position of the optical resonance peak and height of the cylindrical SiNW is weak. With the increase of the height of the cylindrical SiNW, the position of the optical resonance peak redshifts and tends to a fixed value, and its intensity increases. The trend between properties of the optical resonance peak and height of the cylindrical SiNW is the same as that of our previous work [18]. For the trilobal SiNW with two equivalent scales, it has the same trend that the position of optical resonance peak redshifts, and its intensity increases with the increase of the height of the trilobal SiNW. The total light absorption and obtainable J_{SC} of two kinds of SiNWs increase with height of the SiNWs, and the total light absorption and obtainable J_{SC} of the trilobal SiNW are higher than that of the cylindrical SiNW with the same height.

The incident angle is an important factor affecting the light absorption for single-nanowire solar cells. Figures 4(a) and 4(b)

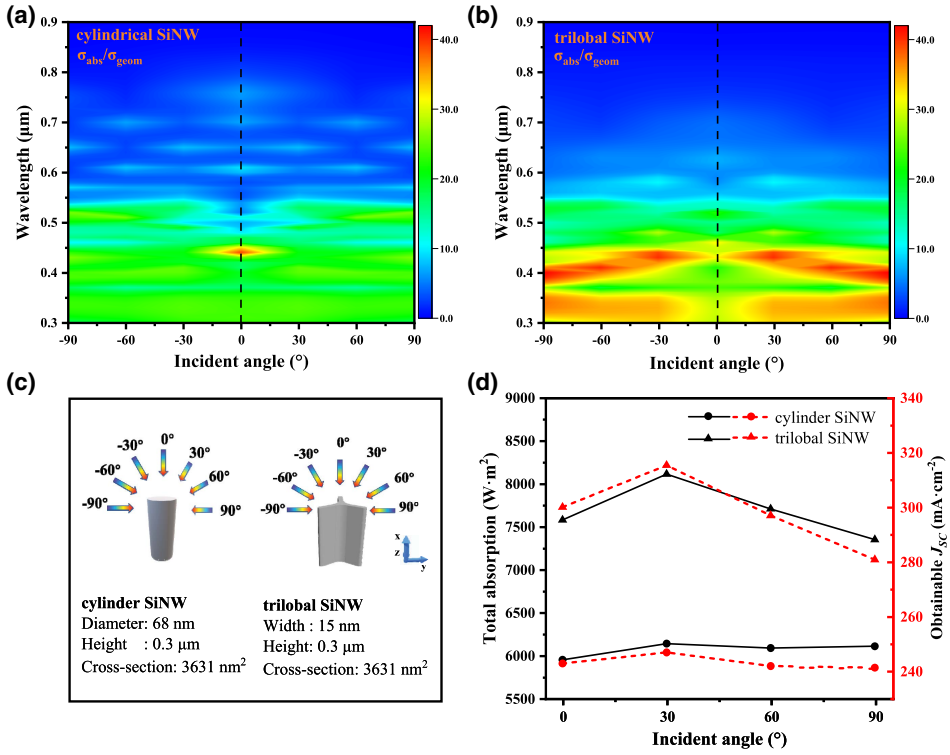

Fig. 4. Absorption efficiency of (a) cylindrical and (b) trilobal SiNWs with different incident angles, (c) diagram of two kinds of SiNWs with different incident angles, and (d) total absorption and obtainable J_{SC} with different incident angles.

show the light-absorption efficiency of two kinds of SiNW with different incident angles. The absorption efficiency spectra have strong symmetry with the change of incident angle due to the symmetry of geometry of two kinds of SiNWs. Therefore, the range of the incident angle of 0°–90° in Fig. 4(c) was analyzed. The intensity of the optical resonance peak at the wavelength of 0.44 μm decreases, and the width of the light-absorption efficiency spectrum increases with the increase of the incident angle in the cylindrical SiNW. The total light absorption and obtainable J_{SC} have little change, and the influence of incident angle on the cylindrical SiNW is little. For the trilobal SiNW, the optical resonance peak blueshifts, and total light-absorption intensity first increases and then decreases with the increase of incident angle. The difference between the maximum and minimum values of total light is 760 $W \cdot m^{-2}$, accounting for 9% of the maximum value, and that of obtainable J_{SC} is 35 $mA \cdot cm^{-2}$, accounting for 11% of the maximum value. The trilobal SiNW also has a good tolerance for the incident angle.

Table 2 shows that the total light absorption of the trilobal SiNW can achieve 15,969 $W \cdot m^{-2}$, which is 4398 $W \cdot m^{-2}$ higher than that of the cylindrical SiNW, about 16 times higher the total irradiance of AM 1.5 G. The best obtainable J_{SC} of the trilobal SiNW is 647 $mA \cdot cm^{-2}$, which is 166 $mA \cdot cm^{-2}$ higher than that of the cylindrical SiNW, about 13 times higher than that of the non-concentrating silicon solar cells. An apparent power conversion efficiency of single trilobal SiNW solar cell will exceed the Shockley–Queisser limit, because the trilobal SiNW with two equivalent scales has absolute advantages in light-capture capability. To obtain the excellent optical

Table 2. Total Light-Absorption Intensity and Obtainable J_{SC} of Trilobal and Cylindrical SiNWs

	Trilobal SiNW		Cylindrical SiNW	
Serial Number	Absorption Intensity[a] ($W \cdot m^{-2}$)	Obtainable J_{SC}[a] ($mA \cdot cm^{-2}$)	Absorption Intensity[a] ($W \cdot m^{-2}$)	Obtainable J_{SC}[a] ($mA \cdot cm^{-2}$)
1	7733	295	6152	252
2	7573	299	5945	242
3	7591	302	5402	219
4	6989	282	5207	210
5	2786	103	2475	96
6	7573	299	5944	242
7	11,846	476	8906	367
8	15,969	647	11,571	481

[a]Data are accurate to the integer bit; the geometric parameters corresponding to the serial number are shown in Table 1.

properties of a single-SiNW solar cell, it is important to overcome the experimental preparation of trilobal SiNWs. The trilobal SiNW can be fabricated by inductively coupled plasma (ICP) etching with the etching mask on Si substrate. And it is found that there are irregular trilobal SiNWs in the SiNW array by the metal-assisted chemical etching method [34]. The trilobal nanowire is expected to further improve the single-nanowire solar cell's efficiency by replacing a cylindrical single nanowire.

4. CONCLUSION

In summary, we designed a trilobal SiNW with two equivalent scales, which is based on the relationship between the diameter, height, and optical resonance peak in the cylindrical SiNW. The electric field is concentrated in the blades with small equivalent scale in the short wavelength range ($\lambda \leq 0.46$ μm) and in the pivot with large equivalent scale in the long wavelength range ($\lambda \geq 0.54$ μm), and there are electric field distractions at both blade and pivot in the medium wavelength range ($0.46\ \mu m \leq \lambda \leq 0.54\ \mu m$). This electric field distribution proves that different equivalent scales correspond to different positions of optical resonance peaks. Meanwhile, the relationship between the geometric parameters and optical resonance was obtained for improving the light-capture capability of the trilobal SiNW. Then the light-absorption capacity and obtainable J_{SC} of the trilobal SiNW are higher than that of the cylindrical SiNW with the same cross section and height. The total light absorption of a single trilobal SiNW can achieve 15,969 $W \cdot m^{-2}$, about 16 times the solar irradiance of AM 1.5 G, and the obtainable J_{SC} can achieve 647 $mA \cdot cm^{-2}$, about 13 times that of non-concentrating silicon solar cells. This work provides a new choice for designing single nanowire with excellent light-capture capability.

APPENDIX A

The Appendix A section includes the absorption efficiency spectra of trilobal SiNW with different polarization directions, as shown in Fig. 5.

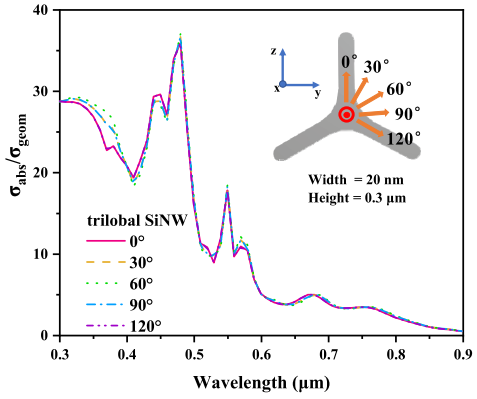

Fig. 5. Absorption efficiency ($\sigma_{abs}/\sigma_{geom}$) spectra of trilobal SiNW with different polarization directions; the illustration shows the polarization directions.

Funding. National Natural Science Foundation of China (51972110, 51772096); Beijing Science and Technology Project (Z181100005118002); Par-Eu Scholars Program; Science and Technology Beijing 100 Leading Talent Training Project; Fundamental Research Funds for the Central Universities (2017ZZD02); NCEPU "Double First-Class" Graduate Talent Cultivation Program.

Disclosures. The authors declare that there are no conflicts of interest related to this paper.

REFERENCES

1. Z. Wang, "ZnO nanowire and nanobelt platform for nanotechnology," Mater. Sci. Eng. **64**, 33–71 (2009).
2. S. Li, J.-P. Chou, H. Zhang, Y. Lu, and A. Hu, "A study of strain-induced indirect–direct bandgap transition for silicon nanowire applications," J. Appl. Phys. **125**, 082520 (2019).
3. G. Yang, T. Takei, S. Yanagida, and N. Kumada, "Hexagonal tungsten oxide-polyaniline hybrid electrodes for high-performance energy storage," Appl. Surf. Sci. **498**, 143872 (2019).
4. A. Sharma, A. Khan, Y. Zhu, R. Halbich, W. Ma, Y. Tang, B. Wang, and Y. Lu, "Quasi-line spectral emissions from highly crystalline one-dimensional organic nanowires," Nano Lett. **19**, 7877–7886 (2019).
5. C. Gutsche, A. Lysov, D. Braam, I. Regolin, G. Keller, Z.-A. Li, M. Geller, M. Spasova, W. Prost, and F.-J. Tegude, "n-GaAs/InGaP/p-GaAs core-multishell nanowire diodes for efficient light-to-current conversion," Adv. Funct. Mater. **22**, 929–936 (2012).
6. P. Krogstrup, H. I. Jørgensen, M. Heiss, O. Demichel, J. V. Holm, M. Aagesen, J. Nygard, and A. Fontcuberta i Morral, "Single-nanowire solar cells beyond the Shockley–Queisser limit," Nat. Photonics **7**, 306–310 (2013).
7. Y. Zhang and H. Liu, "Nanowires for high-efficiency, low-cost solar photovoltaics," Crystals **9**, 87 (2019).
8. B. Tian, X. Zheng, T. J. Kempa, Y. Fang, N. Yu, G. Yu, J. Huang, and C. M. Lieber, "Coaxial silicon nanowires as solar cells and nanoelectronic power sources," Nature **449**, 885–889 (2007).
9. Y. Dong, B. Tian, T. J. Kempa, and C. M. Lieber, "Coaxial group III-nitride nanowire photovoltaics," Nano Lett. **9**, 2183–2187 (2009).
10. A. L. Briseno, T. W. Holcombe, A. I. Boukai, E. C. Garnett, S. W. Shelton, J. J. Frechet, and P. Yang, "Oligo- and polythiophene/ZnO hybrid nanowire solar cells," Nano Lett. **10**, 334–340 (2010).
11. Z. Li, H. H. Tan, C. Jagadish, and L. Fu, "III–V semiconductor single nanowire solar cells: a review," Adv. Mater. Technol. **3**, 1800005 (2018).
12. D. van Dam, N. J. van Hoof, Y. Cui, P. J. van Veldhoven, E. P. Bakkers, J. Gomez Rivas, and J. E. Haverkort, "High-efficiency nanowire solar cells with omnidirectionally enhanced absorption due to self-aligned indium-tin-oxide mie scatterers," ACS Nano **10**, 11414–11419 (2016).
13. J. E. M. Haverkort, E. C. Garnett, and E. P. A. M. Bakkers, "Fundamentals of the nanowire solar cell: optimization of the open circuit voltage," Appl. Phys. Rev. **5**, 031106 (2018).
14. M. D. Ko, T. Rim, K. Kim, M. Meyyappan, and C. K. Baek, "High efficiency silicon solar cell based on asymmetric nanowire," Sci. Rep. **5**, 11646 (2015).
15. S. Bhattacharya and S. John, "Beyond 30% conversion efficiency in silicon solar cells: a numerical demonstration," Sci. Rep. **9**, 12482 (2019).
16. X. Fang, C. Y. Zhao, and H. Bao, "Radiative behaviors of crystalline silicon nanowire and nanohole arrays for photovoltaic applications," J. Quant. Spectrosc. Radiat. Transfer **133**, 579–588 (2014).
17. D. Li and R. Jiao, "Design of a low-filling-factor and polarization-sensitive superconducting nanowire single photon detector with high detection efficiency," Photon. Res. **7**, 847–852 (2019).
18. Y. Li, M. Li, R. Li, P. Fu, B. Jiang, D. Song, C. Shen, Y. Zhao, and R. Huang, "Linear length-dependent light-harvesting ability of silicon nanowire," Opt. Commun. **355**, 6–9 (2015).

19. J. Tong, M. Zhang, S. Zhang, Y. Lei, M. Li, M. Qin, and Y. Li, "Effects of the ambient medium and structure parameter on the optical properties of tapered silicon nanowire," Opt. Commun. **454**, 124515 (2020).
20. Y. Li, L. Yue, Y. Luo, W. Liu, and M. Li, "Light harvesting of silicon nanostructure for solar cells application," Opt. Express **24**, A1075–A1082 (2016).
21. Y. Li, W. Liu, Y. Luo, M. Cui, and M. Li, "Oxidation of silicon nanowire can transport much more light into silicon substrate," Opt. Express **26**, A19–A29 (2018).
22. Y. Li, Y. Luo, W. Liu, M. Cui, J. Kumar, B. Jiang, L. Chu, and M. Li, "Specific distribution of the light captured by silver nanowire," Opt. Express **25**, 9225–9231 (2017).
23. Y. Li, M. Li, R. Li, P. Fu, T. Wang, Y. Luo, J. M. Mbengue, and M. Trevor, "Exact comprehensive equations for the photon management properties of silicon nanowire," Sci. Rep. **6**, 24847 (2016).
24. M. Hussein, "Electrical characteristics of funnel-shaped silicon nanowire solar cells," J. Photon. Energy **7**, 047501 (2017).
25. Y. Li, M. Li, P. Fu, R. Li, D. Song, C. Shen, and Y. Zhao, "A comparison of light-harvesting performance of silicon nanocones and nanowires for radial-junction solar cells," Sci. Rep. **5**, 11532 (2015).
26. S. S. A. Obayya, M. I. Eladawy, R. Mubarak, M. Hussein, M. F. O. Hameed, and F. M. H. Korany, "Conical structures for highly efficient solar cell applications," J. Nanophotonics **12**, 016019 (2018).
27. M. Hussein, M. F. Hameed, N. F. Areed, A. Yahia, and S. S. Obayya, "Funnel-shaped silicon nanowire for highly efficient light trapping," Opt. Lett. **41**, 1010–1013 (2016).
28. B. T. Draine and P. J. Flatau, "Discrete-dipole approximation for scattering calculations," J. Opt. Soc. Am. A **11**, 1491–1499 (1994).
29. B. T. Draine and P. J. Flatau, "Discrete-dipole approximation for periodic targets: theory and tests," J. Opt. Soc. Am. A **25**, 2693–2703 (2008).
30. P. J. Flatau and B. T. Draine, "Fast near field calculations in the discrete dipole approximation for regular rectilinear grids," Opt. Express **20**, 1247–1252 (2012).
31. Y. Li, M. Li, D. Song, H. Liu, B. Jiang, F. Bai, and L. Chu, "Broadband light-concentration with near-surface distribution by silver capped silicon nanowire for high-performance solar cells," Nano Energy **11**, 756–764 (2015).
32. http://rredc.nrel.gov/solar/spectra/am1.5/ASTMG173/ASTMG173.html.
33. N. Anttu, "Absorption of light in a single vertical nanowire and a nanowire array," Nanotechnology **30**, 104004 (2019).
34. F. Bai, M. Li, R. Huang, Y. Yu, T. Gu, Z. Chen, H. Fan, and B. Jiang, "Wafer-scale fabrication of uniform Si nanowire arrays using the Si wafer with UV/ozone pretreatment," J. Nanopart. Res. **15**, 1915 (2013).